



Research article

3D digital analysis of magnetic force-driven orthodontic tooth movement

Yukinori Kuwajima^a, Yoshiki Ishida^a, Cliff Lee^{a,b}, Hisayo Mayama^c, Kazuro Satoh^c, Shigemi Ishikawa-Nagai^{a,*}

^a Department of Oral Medicine, Immunity and Infection, Harvard School of Dental Medicine, Boston, MA, USA

^b Department of Orofacial Sciences, University of California, San Francisco School of Dentistry, CA, USA

^c Division of Orthodontics, Department of Developmental Oral Health Science, School of Dentistry, Iwate Medical University, Morioka, Iwate, Japan



ARTICLE INFO

Keywords:

Dentistry
Dental materials
Medical imaging
Health technology
Magnetic forces
NdFeB magnets
Orthodontic tooth movements
Force control

ABSTRACT

With the introduction of rare earth magnets like neodymium-iron-boron (NdFeB), it has become possible to produce small magnets with high forces, necessary for its usage in the field of dentistry, such as for orthodontic tooth movement. The ultimate goal of this project is to establish magnetic force-driven orthodontic treatment as a future treatment modality for comprehensive orthodontic treatment.

In order to utilize magnets for orthodontic treatment, we must first understand the characteristics of tooth movement created by magnetic forces. In this study, we aimed to digitally assess the efficacy of magnetic attraction and repulsion forces by means of a 3D digital analysis of movement (distance, direction, angulation and duration) and rotation (yaw, pitch and roll) of the crown and root of teeth in an *ex vivo* typodont model. We performed space closure and space gain treatment of maxillary central incisors ($n = 30$) and analyzed the movement and rotation of the teeth and root apex with 3D digital analysis. The results of the typodont model indicated significant differences on amount, speed and rotation of tooth and root movement created by magnetic attraction and repulsion forces.

We also mimicked a moderate crowding typodont case and successfully treated it with a combination of attraction and repulsion magnetic forces. The moderate crowding case utilized magnets and a titanium archwire to guide the planned tooth movements and prevent undesired or unexpected movement. Further *ex vivo* experiments and considerations for biosafety will be necessary to investigate magnet force-driven orthodontics as a future modality of orthodontic treatment.

1. Introduction

Magnets were first used in dentistry in the 1950s for the fixation of prosthodontic and maxillofacial prostheses [1, 2, 3, 4]. In maxillofacial cases with a significant amount of hard and soft tissue removal, due to malignancy or tumor, magnets enable the retention and stability of prosthetics where it would have been difficult and impractical by other means. Intra-oral and extra-oral obturators and prosthetics retained with the use of magnets have allowed for the rehabilitation of facial defects and significantly improved the quality of life for patients [5]. With the introduction of rare earth magnets, such as samarium-cobalt (SmCo) and neodymium-iron-boron (NdFeB), it has become possible to produce smaller magnets with the necessary force for other dental applications, such as orthodontics [6].

The ultimate goal of this project is to establish magnetic force-driven orthodontic treatment as a future treatment modality. Current

orthodontic treatment modalities are 1) conventional fixed orthodontic appliances (FOA) using brackets, arch wires and elastic bands, 2) removable orthodontic clear aligner systems which use clear transparent trays, such as Invisalign®, ClearCorrect® and other similar systems. Weaknesses in these methods are a lack of force continuity and the reliance on patient compliance in wearing the removable trays or elastic bands. Magnetic force-driven orthodontics can address these limitations. There are many advantages of utilizing magnets in orthodontic treatment. The major significant advantages of magnets over traditional force delivery systems are frictionless mechanism, predictable force, and no force decay. Magnets exert continuous forces with no friction, compared with conventional orthodontic appliances and may be used for predictable force control for both attraction and repulsion force [7]. Magnetic forces can be exerted through physical barriers such as mucosa and bone. Furthermore, the magnet force-driven approach does not require patient compliance and cooperation in placing removable components such as

* Corresponding author.

E-mail address: shigemi_nagai@hsdm.harvard.edu (S. Ishikawa-Nagai).

elastic bands or trays. There have been several early studies on the use of magnets for dental and orthodontic use [7, 8, 9, 10, 11, 12, 13, 14, 15, 16, 17]. Darendeliler et al reviewed the clinical applications of magnets in orthodontics, including tooth movement for space closure, molar distalization, and tooth extrusion, as well as in the use of orthopedic appliances for skeletal corrections of malocclusion [10]. They also reported on the biological implications of magnets in the oral cavity, namely with SmCo and NdFeB magnets, with corrosion being the principal limitation in the usage and lifespan of magnets in an oral environment. However, 3-dimensional the tooth and root movement and rotation by the magnet force have never been investigated digitally. Recently, FeCo-(Al-fluoride) nanogranular films exhibiting ferromagnetic properties with high optical transparency in the visible light spectrum have been introduced [18]. With the development of small transparent magnets, comprehensive magnetic force-driven orthodontic has the potential to become the future method of orthodontic treatment.

Another advantage is that static magnetic fields have gained considerable popularity as an alternative therapy for pain relief, especially in chronic pain [19, 20], osteoarthritis pain [21, 22], neuropathic pain [23], and postoperative pain [24]. The widespread adaptation is largely due to the perceived efficacy and safety with minimal side-effects [25, 26]. There is a significant body of research [27, 28, 29] on the inhibition of P2X₃ receptors for relieving inflammatory and neuropathic pain. A recent report revealed that static magnetic field (SMF) was found to reduce pain levels and down-regulate expressions P2X₃ in mice after experimental tooth movement [30]. Pain relief could be an additional benefit of utilizing magnetic force-driven orthodontic treatment.

In order to utilize magnets for orthodontic treatment, we must first understand the characteristics of tooth movement created by magnetic forces. In this study, we first digitally assessed efficacy of magnetic attraction and repulsion forces by means of a 3D digital analysis of movement (distance, direction, angulation and duration) and rotation (yaw, pitch and roll) of the crown and root of a tooth in an *ex vivo* typodont model. Typodont models with teeth embedded in a wax base arranged in malocclusion have been routinely used for pre-clinical orthodontics education and research. In addition, a combination of attraction and repulsion forces was used to treat a moderate crowding typodont case to validate this approach in comprehensive treatment.

2. Materials and methods

2.1. Fabrication of typodont model with magnets and 3D digital scanning

Dental typodonts mimicking maxillary central incisors were used in this *ex vivo* experiment. Dental typodont models of maxillary central incisors (24.0 mm length, 10.0 mm width, and 8.0 mm crown thickness) were designed using CAD software (Creo Elements/Direct Modeling Express 4.0, PTC, Needham, MA, USA). Three 1.5 mm diameter x 1.0 mm height cone-shaped measurement horns were created on the center of the incisal edge, distal and lingual side of the tooth. A shallow groove (2 mm

apicoroonally, 5 mm mesiodistally, 0.5 mm buccolingually) was designed on the labial surface of the tooth to accurately reproduce the positioning of magnet placement (Fig. 1A). A prior pilot study was completed to confirm no significant difference in measurements of tooth movement and rotation with and without labial grooves. The designs were exported as STL files. The tooth models were fabricated using a 3D printer (MiiCraft 125, MiiCraft Inc., Hsinchu, Taiwan) using model resin (Next Dent® Model 2.0, Next Dent BV, Soesterberg, Netherland).

The typodont box (60 mm × 50 mm x 25 mm of outer frame, 30 mm × 30 mm x 20 mm of the inner tub) was designed using the CAD software. One hundred and twelve landmarks (4.0 mm × 1.5 mm pentagonal cones) were created on the surfaces of the typodont boxes (Fig. 1B) in order to superimpose data accurately. Typodont boxes were fabricated in the same manner as the tooth models.

Ni-plated cylindrical NdFeB N52 magnets (NeoMag Co., Ltd., Chiba, Japan, 2.0 mm diameter x 5.0 mm, surface magnetic flux density 414 mT, adsorption power 22 kPa, density 7.5 g/cm³) were used in this *ex vivo* study. The magnets were bonded to the grooves, with the *north* pole of the UL1 (maxillary left central incisor) magnet facing the mesial and the *south* pole of the UR1 (maxillary right central incisor) magnet facing the mesial, to produce an attraction force for the space-closing (SC) model, and the teeth were placed 2 mm apart (Fig. 1B). The opposite setting was used to produce repulsion force for the space-gain (SG) model, with the *north* pole of the UR1 magnet facing the mesial. The teeth were then stabilized in the typodont box using paraffin wax which is normally used for dental typodont (Paraffin wax, GC Co., Ltd., Tokyo, Japan, solidification point 59.3 °C). A plastic guide made with self-curing acrylic resin (Pattern Resin, GC Chicago, IL, USA) was created to standardize tooth position for 30 typodonts.

The typodonts were scanned using a 3D laser scanner (Ortho Insight 3D® Laser Scanner, Motion View LLC., Chattanooga, TN, USA) prior to tooth movement. The typodonts were positioned in the center of the scanning table with the magnet facing the front and scanned. After the initial scan, the typodonts were divided into 10 groups, with 3 typodonts in each group for a total of 30 typodonts. The typodonts were immersed in a digital thermostatic water bath (Joan Lab Digital Thermostatic Water Bath Manufacturer, Ningbo Yinzhou Joan Lab Equipment Co., Ltd., Zhejiang, China, 3 L capacity) to initiate tooth movement at 55 °C for 5 min up to 50 min in increments of 5 min depending on the group. After complete immersion of the typodont model in the water bath for the prescribed time, the models were stabilized in a cold-water bath at 5 °C for 30 min. Immediately after the completion of immersion of typodont model, excess water around the model was removed gently using compressed air and the models were scanned in the same manner as the initial scans.

The scanned typodont model data was converted to STL files using 3D visualization software (Ortho Insight 3D®, Motion View LLC., Chattanooga, TN, USA). The pre-movement STL files were superimposed on the post-movement using 3D data inspection software (GOM inspect, GOM, Braunschweig, Germany) using the 112 landmarks on the typodont box.

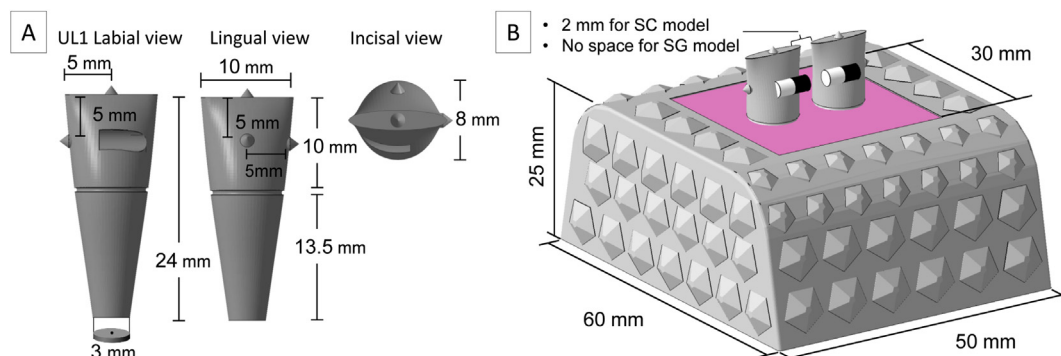


Fig. 1. Experiment models. (A) Design and sizes of UL1, (B) Scheme of typodont model.

3D coordinates (X, Y, Z axis) of each of the 3 measurement points on the tooth model of UR1 and UL1 were obtained (Fig. 2A). 3D coordinates (X, Y, Z axis) of the center of root apex (CRA, Fig. 2B) of UR1 and UL1 were obtained by superimposing designed tooth model on the crown portion of typodont model.

2.2. Analysis of the movement and rotation of tooth crown portion

The center of gravity (CG) of each tooth crown was calculated using 3D coordinates of 3 measurement points by the following Eq. (1).

$$CG(x) = \frac{X_1 + X_2 + X_3}{3} \quad CG(y) = \frac{Y_1 + Y_2 + Y_3}{3} \quad CG(z) = \frac{Z_1 + Z_2 + Z_3}{3} \quad (1)$$

The amount of 3D movement of the CG of each tooth crown portion (ACG) in each of 10 time-series was calculated by the following Eq. (2):

$$\begin{aligned} ACG - X (UR1, UL1) &= CG (x) - Post (UR1, UL1) - CG (x) - Pre (UR1, UL1) \\ ACG - Y (UR1, UL1) &= CG (y) - Post (UR1, UL1) - CG (y) - Pre (UR1, UL1) \\ ACG - Z (UR1, UL1) &= CG (z) - Post (UR1, UL1) - CG (z) - Pre (UR1, UL1) \end{aligned} \quad (2)$$

The speed of X-axis movement (mm/min) at time points of 5, 15, 25, 35, and 45min were calculated, using ACG by the following Eq. (3):

$$Speed (mm/min) = [ACG (t) - ACG (t - 5)] / 5 \quad (3)$$

where ACG(t) is the amount of 3D movement of CG in the duration of t minutes. The average moving speeds on SC and SG model were compared.

The distance between UR1 and UL1 on the CG of each tooth crown (DCG) was calculated by the following Eq. (4):

$$DCG = \sqrt{(CG(x)_{UR1} - CG(x)_{UL1})^2 + (CG(y)_{UR1} - CG(y)_{UL1})^2 + (CG(z)_{UR1} - CG(z)_{UL1})^2} \quad (4)$$

$$\begin{aligned} ACRA - X (UR1, UL1) &= CRA (x) - Post (UR1, UL1) - CRA (x) - Pre (UR1, UL1) \\ ACRA - Y (UR1, UL1) &= CRA (y) - Post (UR1, UL1) - CRA (y) - Pre (UR1, UL1) \\ ACRA - Z (UR1, UL1) &= CRA (z) - Post (UR1, UL1) - CRA (z) - Pre (UR1, UL1) \end{aligned} \quad (10)$$

Description of 3D rotation, yaw, pitch, and roll are shown in Fig. 3. When given two cartesian coordinates, we can calculate the rotation using the dot and cross of the two vectors following Eqs. (5) and (6). The cross product will be used as the normal axis (n), and dot product will show the angle (θ) of the rotation.

$$n = a \times b \quad (5)$$

$$a \cdot b = \|a\| \|b\| \cos(\theta) \quad (6)$$

From the angle and the axis, it is possible to construct the rotation matrix (R) by using Rodrigues' rotation formula [31] (7) below.

$$R_n(\theta) = \begin{bmatrix} \cos \theta + n_x^2(1 - \cos \theta) & n_x n_y(1 - \cos \theta) - n_z \sin \theta & n_x n_z(1 - \cos \theta) + n_y \sin \theta \\ n_y n_x(1 - \cos \theta) + n_z \sin \theta & \cos \theta + n_y^2(1 - \cos \theta) & n_y n_z(1 - \cos \theta) - n_x \sin \theta \\ n_z n_x(1 - \cos \theta) - n_y \sin \theta & n_z n_y(1 - \cos \theta) + n_x \sin \theta & \cos \theta + n_z^2(1 - \cos \theta) \end{bmatrix} \quad (7)$$

There are several ways to show the rotational transition, we use the yaw (Z-axis), pitch (X-axis), and roll (Y-axis) angles.

$$\begin{bmatrix} \cos \beta \cos \alpha & \sin \gamma \sin \beta \cos \alpha - \cos \gamma \sin \alpha & \sin \gamma \sin \alpha + \cos \gamma \sin \beta \cos \alpha \\ \cos \beta \sin \alpha & \sin \gamma \sin \beta \sin \alpha + \cos \gamma \cos \alpha & -\sin \gamma \cos \alpha + \cos \gamma \sin \beta \sin \alpha \\ -\sin \beta & \sin \gamma \cos \beta & \cos \gamma \cos \beta \end{bmatrix} \quad (8)$$

Given the rotation matrix (8), we can derive gamma, beta, alpha from the following Eq. (9):

$$\begin{aligned} R_{31} &= -\sin \beta \\ R_{32} &= \sin \gamma \cos \beta \\ R_{33} &= \cos \gamma \cos \beta \end{aligned} \quad (9)$$

2.3. Analysis of the movement of center of root apex

Amount of 3D movement of the CRA (Fig. 2B) of each root (ACRA) in each of 10 time-series of SC models was calculated by the following Eq. (10):

The distance between UR1 and UL1 on the center of root apex (DCRA) was calculated using 3D coordinate of CRA by the following Eq. (11):

$$DCRA = \sqrt{(CRA(x)_{UR1} - CRA(x)_{UL1})^2 + (CRA(y)_{UR1} - CRA(y)_{UL1})^2 + (CRA(z)_{UR1} - CRA(z)_{UL1})^2} \tag{11}$$

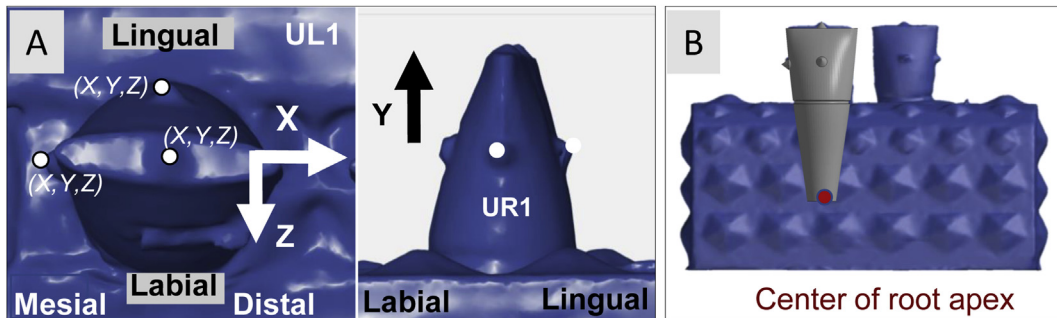


Fig. 2. Explanations of tooth movements and rotations. (A) X, Y and Z axis direction of tooth movement, (B) Identification of center or root apex.

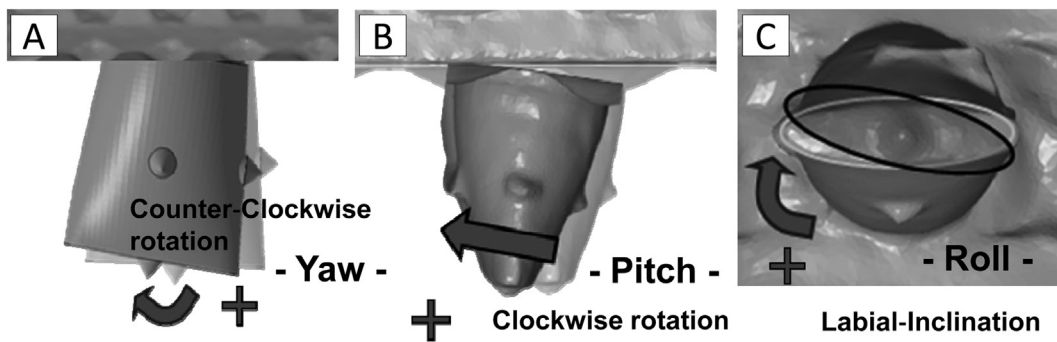


Fig. 3. Explanations of tooth rotations, (A) yaw, (B) pitch and (C) roll.

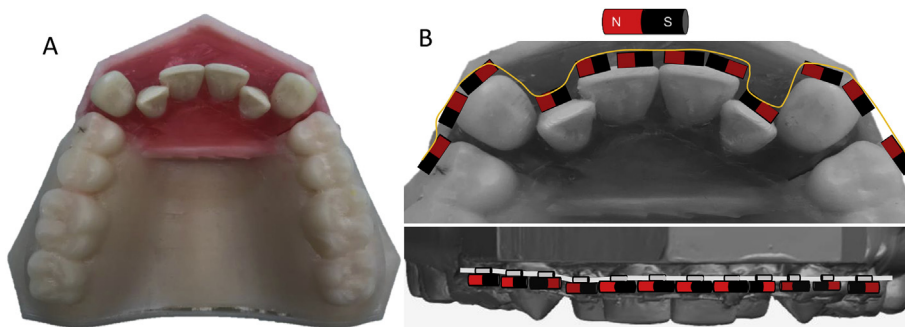


Fig. 4. Application of attraction and repulsion force to the moderate crowding case in ex vivo. (A) Typodont model of a moderate crowding case including teeth #6–11. (B) Magnets setting for attraction and repulsion force.

2.4. Application of attraction and repulsion force to the moderate crowding case

A moderate crowding case including teeth UR3 to UL3 was created in the typodont model and the magnets were placed to setup both attraction and repulsion force to straighten the arch form (Fig. 4). The attraction magnet force was placed in 5 areas (UR4 mesial – UR3 distal, UR2 mesial – UR1 distal, UR1 mesial – UL1 mesial, UL1 distal – UL2 mesial, UL3 distal – UR4 mesial) and repulsion force was placed in 2 areas (#6M-#7D

and #10D-#11M). A nickel-titanium archwire, 0.012 inch Sentalloy® (TOMY INTERNATIONAL INC., Tokyo, Japan) was used as to guide the movement and establish the desired arch form. The model was scanned pre and post-movement and 3D movement and rotation was analyzed in the same manner.

Crown and root movement, crown rotation, and crown speed were obtained and averaged in each of 10 time-series and average data was used for the statistical analysis with one-way analysis of variance (ANOVA), Tukey post-hoc test, and two-tailed Student's t-test. Linear

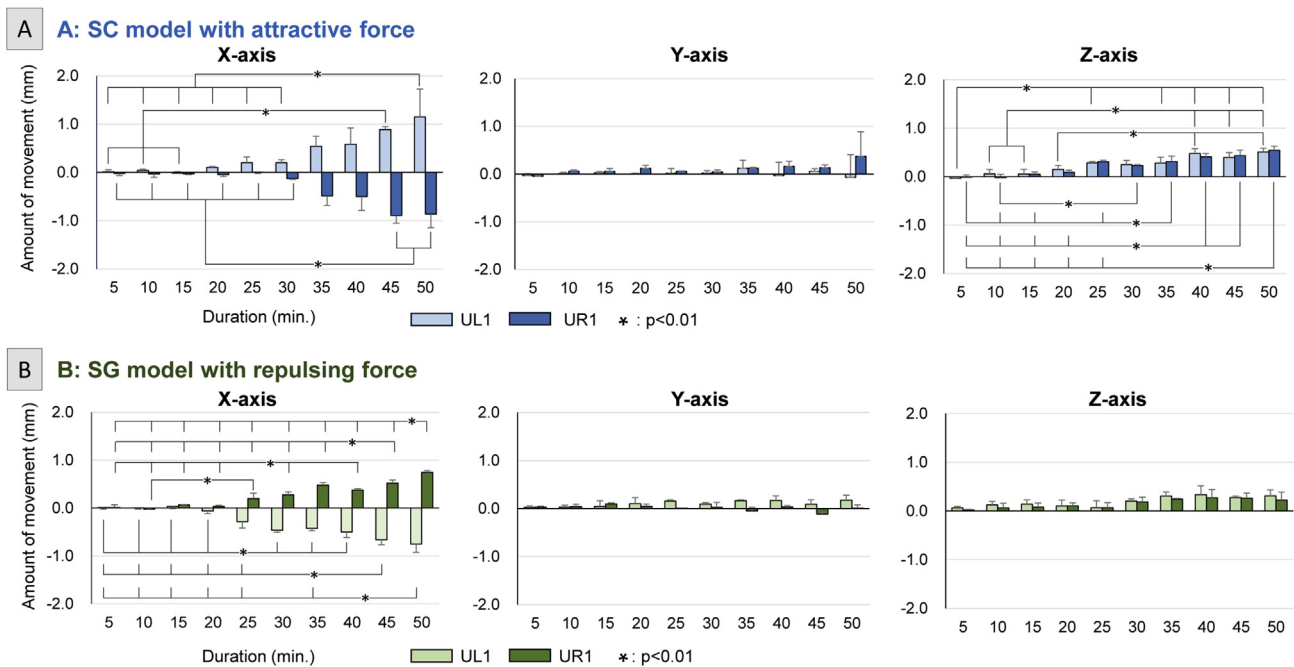


Fig. 5. Amount of movement on center of gravity of UR1 and UL1. (A) SC model, (B) SG model.

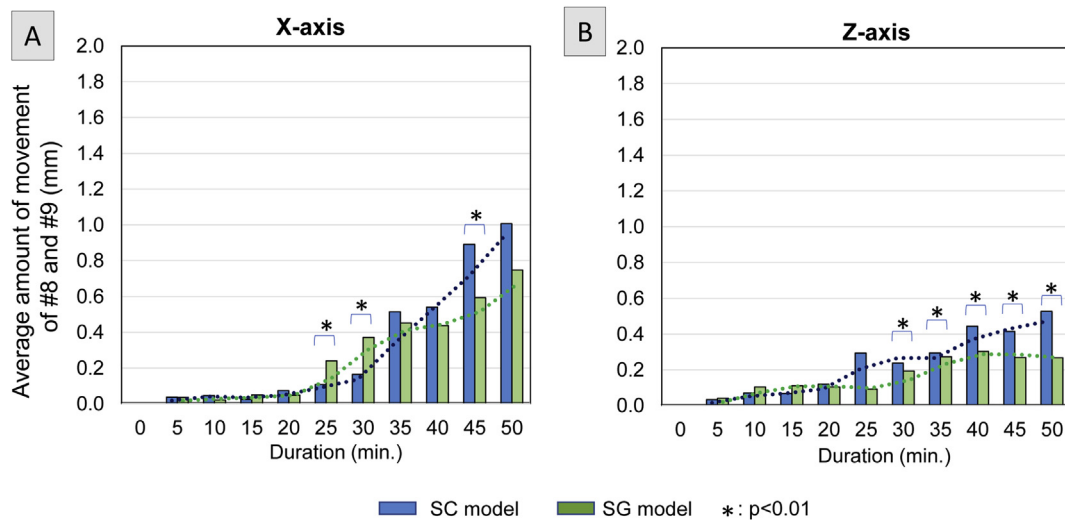


Fig. 6. Comparison of average amount of movement on UR1 and UL1 between SC and SG models. (A) X-axis, (B) Z-axis.

correlation between the crown and root movement were analyzed with Pearson's *r*.

3. Results

3.1. Analysis of coronal tooth 3D movement and rotation

3.1.1. Movement in X, Y and Z axis

The average amount of movement of CG in each of the 3 axes of SC and SG models are shown in Fig. 5. For the SC model (Fig. 5A), X-axis tooth movement on both UR1 and UL1 started after 30 min and continued until 50 min, when the mesial surface of UR1 and UL1 contacted. At 50 min, there was no significant difference between the X-axis movement of UR1 and UL1, with an average movement of -0.86 ± 0.28 mm and 1.15 ± 0.57 mm, respectively. For the Z-axis movement, both UR1 and UL1 moved toward the labial. Significant tooth movements started after 25 min and average of Z-axis movement at 50 min for UR1

and UL1 was 0.54 ± 0.08 mm, 0.51 ± 0.07 mm, respectively, with no significant difference between the two. Y-axis movement (intrusion - extrusion) was rarely observed in all time-series for both UR1 and UL1.

For the SG model (Fig. 5B), X-axis tooth movement on both UR1 and UL1 started after 20 min, the average X-axis movement for UR1 and UL1 was 0.74 ± 0.03 mm and -0.75 ± 0.17 mm, respectively with no significant difference. Similar to SC model, Z-axis movement was smaller than X-axis movement and the average was 0.2 mm–0.3 mm though the time-series. Y-axis movement was rarely observed in all time-series for both UR1 and UL1.

In a comparison of the average amount of X-axis tooth movement of UR1 and UL1 between the SC and SG models, the repulsion force in the SG model had movement that began earlier than in the SC model (Fig. 6A). The attraction force, and amount of movement in the SG model was significantly greater than the SC model at 25min and 30min. However, the total amount of movement in the SG model was significantly smaller than the SC model at 45min (Fig. 6A, $p < 0.01$). In the Z-axis the SC

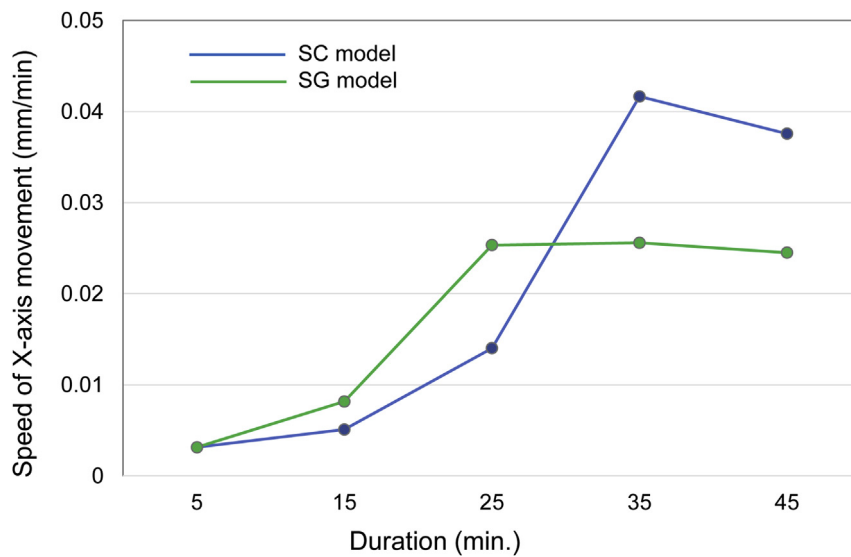


Fig. 7. Comparison of average amount of movement on UR1 and UL1 between SC and SG models.

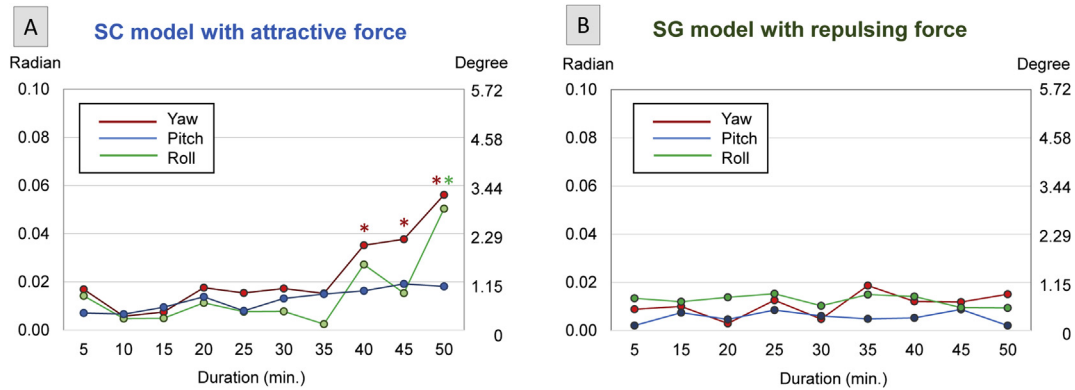


Fig. 8. Amount of tooth rotation. (A) SC model, (B) SG model.

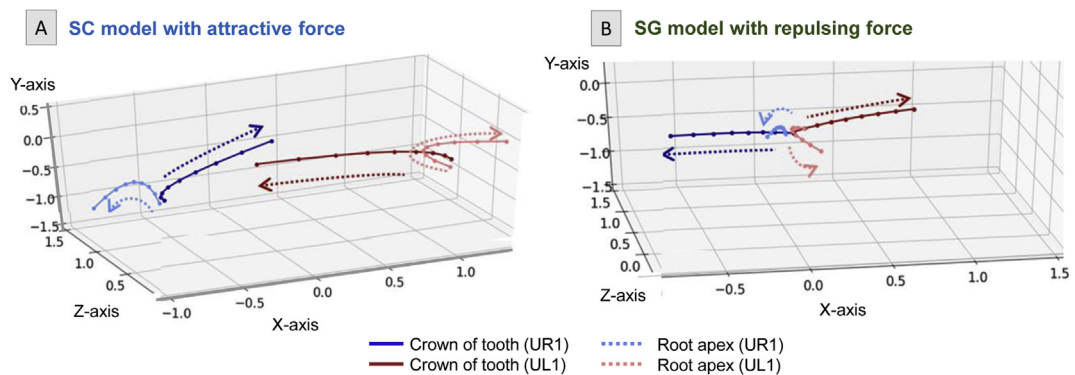


Fig. 9. Trace lined of 3D movement of CG and CRA on UR1 and UL1. (A) SC model, (B) SG model.

model had greater tooth movement than the SG model with significantly greater movement than the SG model at 30min–50min (Fig. 6B, $p < 0.01$).

3.1.2. Speed of movement

The average speed of movement increased exponentially in the SC model before plateauing, whereas the speed increased more linearly in the SG model before plateauing and becoming constant (Fig. 7). The maximum speed reached in the SC model, with attraction force, was

approximately 1.5 times greater than the repulsion force in the SG model.

3.1.3. 3D rotation

In the SC model, significant mesial yaw was observed at the time-series of 40, 45, 50 min (Fig. 8A, $p < 0.01$). Average roll at 50 min was 0.05 radians (2.86°) and it was significantly higher than other time points (Fig. 8A). No significant pitch was observed (Fig. 8A). In the SG model, slight yawing, pitching and rolling were observed throughout (Fig. 8B).

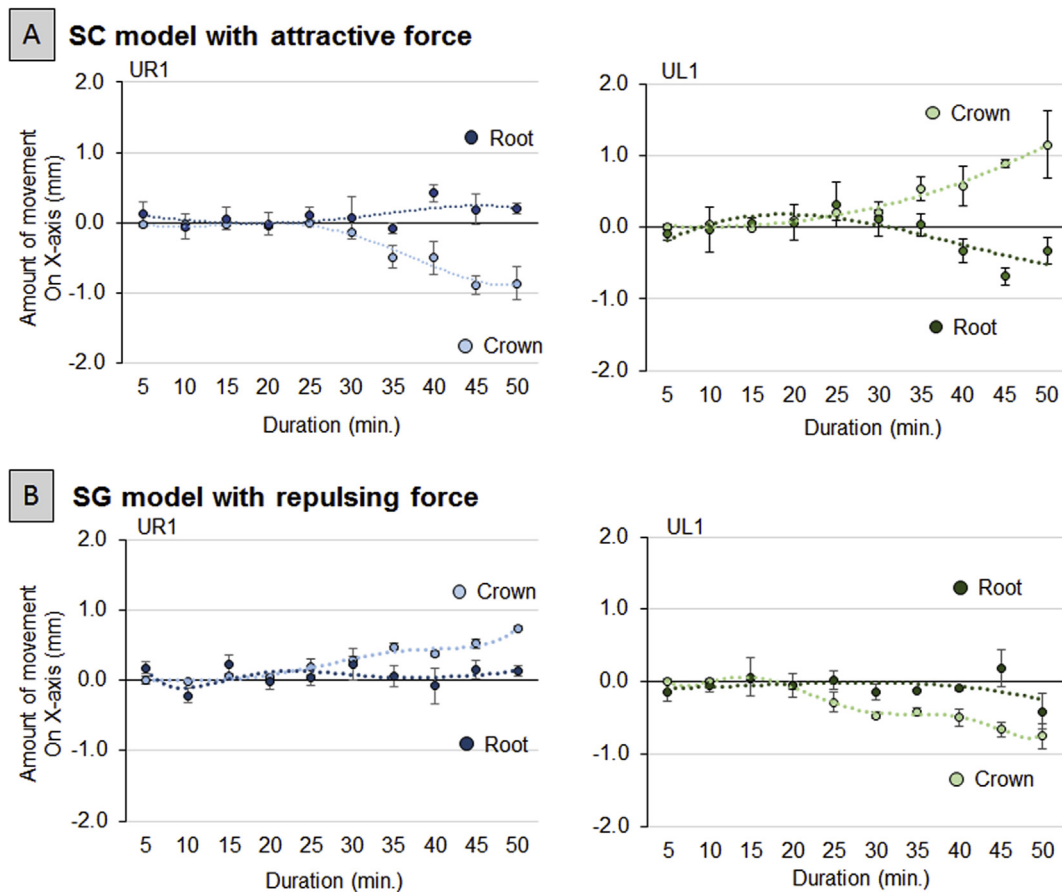


Fig. 10. Correlation of movement between crown and root on X-axis. (A) SC model, (B) SG model.

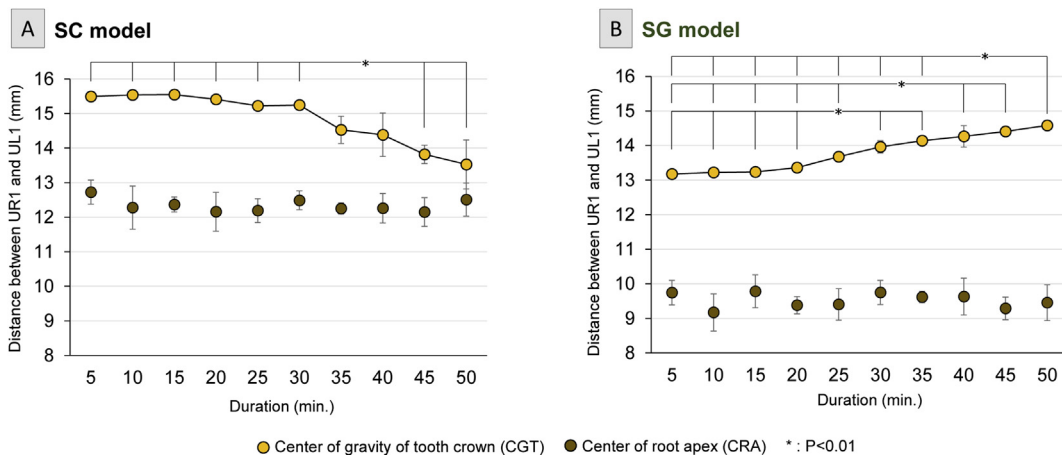


Fig. 11. Distance between UR1 and UL1 on center of gravity tooth crown, and center of root apex. (A) SC model, (B) SG model.

3.2. Comparison of movement of crown of tooth and root apex

3.2.1. Trace line of the 3D movement of the coronal aspect and the root apex of teeth UR1 and UL1

The trace lines of the 3D movement of CG and CRA on UR1 and UL1 are plotted in Fig. 9. In the SC model, as the crowns of the teeth moved mesially to close the space, the root apex moved distally, causing the crown to tip (Fig. 9A). In the SG model, the root apex movement followed the direction of the coronal portion of the teeth (Fig. 9B).

3.2.2. Correlation between X-axis movement on crown of tooth and root apex

A negative correlation was observed on the SC model with attraction force between the X-axis movement of crown and root apex. Pearson's correlation coefficient was -0.2 on UR1 and -0.4 on UL1 respectively (Fig. 10A). In contrast, SG model had a positive correlation ($r = 0.3$) between the X-axis movement of crown and root apex (Fig. 10B).

3.2.3. Distance changes by attraction force and repulsion force

Significant continuous changes on distance between 2 teeth (UR1 and

UL1) was observed. The distance between the two teeth decreased by attraction force in SC model (Fig. 11A) and increased for SG model (Fig. 11B). In contrast, no significant change was observed on the distance between root apex (DCRA) of UR1 and UL1 (Fig. 11A and B).

3.3. Efficacy of magnet force-driven orthodontics tooth movement on moderate crowding case in ex vivo

The crowding arch was straightened in 30 min in the typodont model. 3D scanning data indicated (Table 1, Fig. 12) substantial movement of the crown and root apex on X-axis (mesial-distal movement) and the Z-axis (labial-lingual) on UR3, UR2, UL2, and UL3 as planned. Y-axis movement was rarely observed. Movement of the root apex was observed along with crown movement on UR3, UR2, UL2, and UL3. The repulsion force between UR1 and UL1 mesial stabilized the position, and no significant movement was observed of the crown or root apex. Teeth UR3, UR2, UL2, and UL3 had significant movement and rotation. UR2 and UL2 had yaw and pitch rotation along with major Z-axis movement. In contrast, UR3 and UL3 had pitch and roll rotation along with X-axis movement.

Table 1
3D data on the tooth movement by magnetic force.

3D Movement (mm)						
Tooth #	Crown			Root		
	X-axis	Y-axis	Z-axis	X-axis	Y-axis	Z-axis
UR3	-1.17	0.05	-0.61	0.40	0.03	0.01
UR2	0.34	0.55	2.66	-0.27	0.89	-0.77
UR1	0.17	-0.08	1.08	0.14	-0.05	-0.61
UL1	-0.10	0.05	0.91	0.12	0.08	-0.37
UL2	0.33	0.03	3.53	-0.79	0.46	-0.79
UL3	1.71	-0.02	-1.33	-0.69	0.05	0.48

Rotation of crown (Degree)			
Tooth #	Yaw	Pitch	Roll
UR3	-2.53	-9.82	6.66
UR2	9.07	6.02	1.44
UR1	4.12	1.04	0.34
UL1	3.06	0.75	0.21
UL2	11.05	-3.13	0.74
UL3	-3.90	6.07	4.23

4. Discussion

Force control is the critical factor in orthodontic tooth movement. Force control implies control of the degree, duration, distribution, and direction of force [32]. Magnets have significant advantages over other conventional orthodontic appliances for tooth movement. Magnets produce an operator-controlled, continuous measured force, in both attraction and repulsion, and the forces can be directed and exerted through the surrounding tissue, including mucosa and bone, without any friction or reduction of force. Another advantage of magnet force-driven orthodontics is that the constant force of magnets allows for an auxiliary free orthodontic force system. This contrasts with conventional FOA, where patients have to replace auxiliaries such as orthodontic bands frequently after every meal and with each brushing. To date, orthodontic tooth movement by either conventional appliance or magnetic force has never been fully analyzed objectively using 3D digital technology. This study utilized a 3D digital analysis of tooth movement directed by magnets for the first time.

The magnet size was designed to be used in the maxillary anterior where esthetics are important. A cylindrical shape with a 2 mm diameter and 5 mm length, which can be placed in the labial-cervical area was created. Previous clinical reports used different sized magnets such as 5 mm x 4 mm x 3 mm for mid-line diastema [33], 5 mm diameter with 1 mm thickness and 5 mm x 3 mm for forced orthodontic tooth eruption [13, 14], and 5 mm diameter with 0.75 mm thickness for pre-molar movement [34]. The degree of magnetic force used also varied depending on the study. In order to determine the degree of magnetic force necessary, the expected distance of tooth movement as well as biological safety need to be taken into account. The magnet force we used in this typodont study was 2.2 N is adequate for a 3 mm distance and is about 1/5 of the force, defined by the WHO, as biologically safe [13, 35].

In clinical practice, tooth movement does not start immediately after the application of orthodontic force. This is period of stagnation is due to the time that is necessary for a biological response to the orthodontic forces to begin. Expression and recruitment of different cytokines and osteoclasts due to the appearance of osteoclasts and various cytokines occurs before movement can begin. The plasticity, melting temperature, solidification point of the paraffin wax used for the typodont model helps to mimic this tooth movement in ex vivo setting, however it cannot be directly translated to clinical applications, as the movement achieved in this study would likely require much more time with slower movement in a clinical setting.

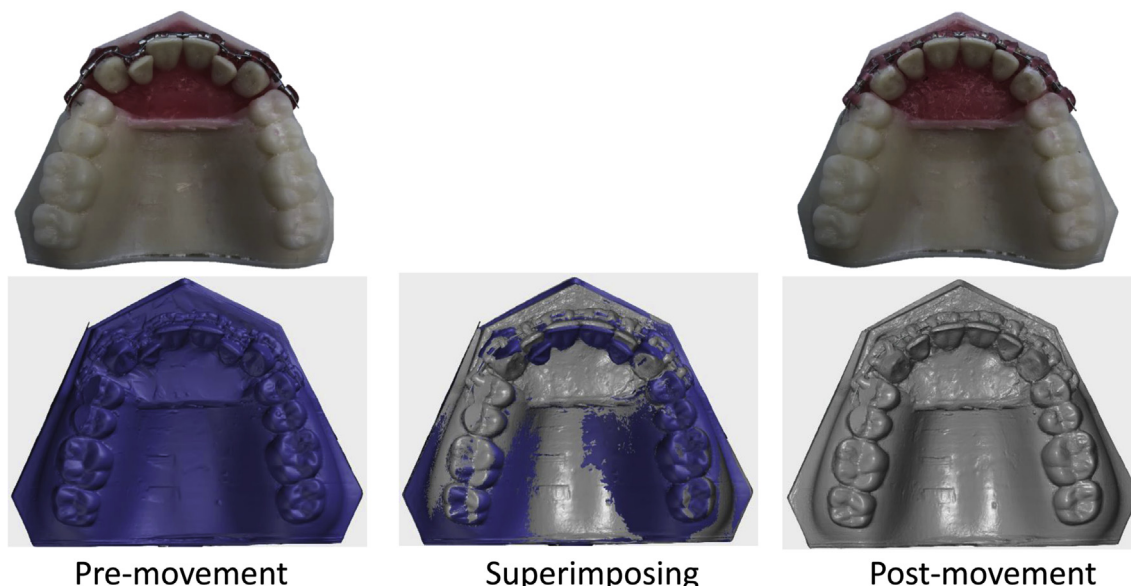


Fig. 12. Typodont model of a moderate crowding case pre- and post-movement.

Our 3D data analysis on attraction and repulsion force for tooth movement provided useful interpretative information for future development of magnetic force-driven orthodontics. The exponential increase of the speed of tooth movement was expected in the SC model; as the spaces close, the magnets get closer together creating a higher attraction force. In contrast, the SG model did not have the inverse pattern. This would have been expected by the inverse square law. If sufficient time were allowed for the teeth to continue moving, and the distance between the magnets increased, the speed and repulsion forces would decrease. The attraction force created larger tooth movement than the repulsion force with a higher maximum speed within 50 min, in 2 mm distance and the same *ex vivo* environment. The attraction force also created more unwanted rotational movements and tipping of the crown with the root apex moving in the opposite direction, a phenomenon not seen in the SG model with the repulsion force. In addition, bodily movement is more desirable in orthodontics, therefore these movements need to be studied further.

Understanding SC/SG findings led to planning the magnet placement in for the moderate crowding case with the use of brackets and an arch wire to allow movement and rotation of teeth UR3-UL3 into their correct location in the arch. The movement occurred as planned without undesired or unexpected movement. The arch wire was instrumental for moving and rotating multiple teeth with precise three-dimensional force control and its significance cannot be understated.

The biggest limitation of this study is that it is a tyodont model in an *ex vivo* setting. One significant limitation of an *ex vivo* environment is the lack of interaction of oral fluids on the magnet, such as potential corrosion. Darendeliler et al summarized biological implications of magnet use in dentistry and corrosion was one of key factors that limited the lifespan and use of magnets in the oral cavity [10]. However, new coatings have been developed to combat corrosion, such as nickel/alumina composite coatings and multilayer titanium nitride ceramic coatings, as well as the development of corrosion resistant magnets, such as iron-platinum (FePt) magnets [36]. Tooth movement *in vivo* is also much more complex than can be simulated in this tyodont model, such as the biological responses to the force of tooth movement. Further research is required such as animal studies and analysis by the finite element method to apply the methods in this study to a clinical situation. With the application of these newer advances, the implementation of magnetic driven orthodontic tooth movement *in vivo* may be achieved.

5. Conclusion

The 3D data obtained in this study validates the use of magnetic force-driven orthodontics in an *ex vivo* setting. Magnets were able to achieve desired tooth movements in a space-closing and space-gain. Future *ex vivo* studies will be needed to optimize and improve the planning and treatment of more complex cases so that they may be implemented in *in vivo*.

Declarations

Author contribution statement

S. Ishikawa-Nagai: Conceived and designed the experiments; Wrote the paper.

K. Satoh: Conceived and designed the experiments.

Y. Kuwajima: Performed the experiments; Analyzed and interpreted the data; Wrote the paper.

Y. Ishida: Performed the experiments; Analyzed and interpreted the data.

C. Lee: Analyzed and interpreted the data; Contributed reagents, materials, analysis tools or data.

H. Mayama: Analyzed and interpreted the data.

Funding statement

This research did not receive any specific grant from funding agencies in the public, commercial, or not-for-profit sectors.

Competing interest statement

The authors declare no conflict of interest.

Additional information

No additional information is available for this paper.

References

- [1] I.M. Thompson, Magnetism as an aid to a prosthetic problem, *Br. J. Oral Surg.* 2 (1) (1964) 44–46.
- [2] J. Nadeau, Maxillofacial prosthesis with magnetic stabilizers, *J. Prosthet. Dent* 6 (1) (1956) 114–119.
- [3] J. Robinson, Magnets for the retention of a sectional intraoral prosthesis: a case history, *J. Prosthet. Dent* 13 (6) (1963) 1167–1171.
- [4] N. Javid, The use of magnets in a maxillofacial prosthesis, *J. Prosthet. Dent* 25 (3) (1971) 334–341.
- [5] S.M. Kim, Magnet-retained orbital prosthesis using a dental implant, *J. Craniofac. Surg.* 28 (2) (2017) e151–e152.
- [6] L. Bondemark, J. Kurol, Distalization of maxillary first and second molars simultaneously with repelling magnets, *EJO (Eur. J. Orthod.)* 14 (4) (1992) 264–272.
- [7] M. Muller, The use of magnets in orthodontics: an alternative means to produce tooth movement, *EJO (Eur. J. Orthod.)* 6 (4) (1984) 247–253.
- [8] A.M. Blechman, H. Smiley, Magnetic force in orthodontics, *Am. J. Orthod.* 74 (4) (1978) 435–443.
- [9] A.M. Blechman, Magnetic force systems in orthodontics: clinical results of a pilot study, *Am. J. Orthod.* 87 (3) (1985) 201–210.
- [10] M.A. Darendeliler, A. Darendeliler, M. Mandurino, Clinical application of magnets in orthodontics and biological implications: a review, *EJO (Eur. J. Orthod.)* 19 (4) (1997) 431–442.
- [11] L. Bondemark, J. Kurol, A.L. Hallonsten, J.O. Andreasen, Attractive magnets for orthodontic extrusion of crown-root fractured teeth, *Am. J. Orthod. Dentofacial Orthop.: Off. Publ. Am. Assoc. Orthod. Const. Soc. Am. Board Orthod.* 112 (2) (1997) 187–193.
- [12] J.H. Noar, R.D. Evans, Rare earth magnets in orthodontics: an overview, *Br. J. Orthod.* 26 (1) (1999) 29–37.
- [13] M. Oki, Y. Yamamoto, T. Yasunaga, R. Shiina, S. Kawano, A. Nakasima, A treatment method for bringing an impacted tooth into the dental arch using fine magnets—measurements of traction force using NdFeB magnets, *J. Jpn. Orthod. Soc.* 60 (2001) 104–111.
- [14] B.O. Cole, A.J. Shaw, R.S. Hobson, et al., The role of magnets in the management of unerupted teeth in children and adolescents, *Int. J. Paediatr. Dent.* 13 (3) (2003) 204–207.
- [15] M.A. Darendeliler, A. Zea, G. Shen, H. Zoellner, Effects of pulsed electromagnetic field vibration on tooth movement induced by magnetic and mechanical forces: a preliminary study, *Aust. Dent. J.* 52 (4) (2007) 282–287.
- [16] W. Hahn, J. Fricke, S. Fricke-Zech, A. Zapf, R. Gruber, R. Sadat-Khonsari, The use of a neodymium-iron-boron magnet device for positioning a multi-stranded wire retainer in lingual retention—a pilot study in humans, *Eur. J. Orthod.* 30 (5) (2008) 433–436.
- [17] M. Sakata, Y. Yamamoto, N. Imamura, S. Nakata, A. Nakasima, The effects of a static magnetic field on orthodontic tooth movement, *J. Orthod.* 35 (4) (2008) 249–254.
- [18] N. Kobayashi, H. Masumoto, S. Takahashi, S. Maekawa, Optically transparent ferromagnetic nanogranular films with tunable transmittance, *Sci. Rep.* 6 (2016) 34227.
- [19] C.S. Brown, F.W. Ling, J.Y. Wan, A.A. Pilla, Efficacy of static magnetic field therapy in chronic pelvic pain: a double-blind pilot study, *Am. J. Obstet. Gynecol.* 187 (6) (2002) 1581–1587.
- [20] S. Kanai, N. Taniguchi, H. Okano, Effect of magnetotherapeutic device on pain associated with neck and shoulder stiffness, *Altern. Ther. Health Med.* 17 (6) (2011) 44–48.
- [21] N.A. Segal, Y. Toda, J. Huston, et al., Two configurations of static magnetic fields for treating rheumatoid arthritis of the knee: a double-blind clinical trial, *Arch. Phys. Med. Rehabil.* 82 (10) (2001) 1453–1460.
- [22] T. Harlow, C. Greaves, A. White, L. Brown, A. Hart, E. Ernst, Randomised controlled trial of magnetic bracelets for relieving pain in osteoarthritis of the hip and knee, *BMJ Br. Med. J. (Clin. Res. Ed.)* 329 (7480) (2004) 1450–1454.
- [23] M.I. Weintraub, G.I. Wolfe, R.A. Barohn, et al., Static magnetic field therapy for symptomatic diabetic neuropathy: a randomized, double-blind, placebo-controlled trial, *Arch. Phys. Med. Rehabil.* 84 (5) (2003) 736–746.
- [24] D. Man, B. Man, H. Plosker, The influence of permanent magnetic field therapy on wound healing in suction lipectomy patients: a double-blind study, *Plast. Reconstr. Surg.* 104 (7) (1999) 2261–2266, discussion 2267–2268.

- [25] N.K. Eccles, A critical review of randomized controlled trials of static magnets for pain relief, *J. Altern. Complement. Med.* 11 (3) (2005) 495–509.
- [26] G. Salomonowitz, M. Friedrich, B. Güntert, Medizinische Relevanz von Magnetfeldern zur Schmerztherapie, *Der Schmerz* 25 (2) (2011) 157–165.
- [27] J. Barclay, S. Patel, G. Dorn, et al., Functional downregulation of P2X3 receptor subunit in rat sensory neurons reveals a significant role in chronic neuropathic and inflammatory pain, *J. Neurosci. : Off. J. Soc. Neurosci.* 22 (18) (2002) 8139–8147.
- [28] P. Honore, K. Kage, J. Mikusa, et al., Analgesic profile of intrathecal P2X₃ antisense oligonucleotide treatment in chronic inflammatory and neuropathic pain states in rats, *Pain* 99 (1-2) (2002) 11–19.
- [29] M.F. Jarvis, E.C. Burgard, S. McGaraughty, et al., A-317491, a novel potent and selective non-nucleotide antagonist of P2X₃ and P2X_{2/3} receptors, reduces chronic inflammatory and neuropathic pain in the rat, *Proc. Natl. Acad. Sci. U.S.A.* 99 (26) (2002) 17179–17184.
- [30] Y. Zhu, S. Wang, H. Long, et al., Effect of static magnetic field on pain level and expression of P2X₃ receptors in the trigeminal ganglion in mice following experimental tooth movement, *Bioelectromagnetics* 38 (1) (2017) 22–30.
- [31] R. Olinde, Des lois géométriques qui régissent les déplacements d'un système solide dans l'espace, et de la variation des coordonnées provenant de ces déplacements considérées indépendamment des causes qui peuvent les produire, *J. Math. Pures Appl.* 5 (1840) 380–440.
- [32] M.M. Stoner, Force control in clinical practice: I. An analysis of forces currently used in orthodontic practice and a description of new methods of contouring loops to obtain effective control in all three planes of space, *Am. J. Orthod.* 46 (3) (1960) 163–186.
- [33] M. Prasad, M. Manoj-Kumar, S. Gowri-Sankar, N. Chaitanya, G. Vivek-Reddy, N. Venkatesh, Clinical evaluation of neodymium-iron-boron (NdFe14B) rare earth magnets in the treatment of mid line diastemas, *J. Clin. Exp. Dent.* 8 (2) (2016) e164–171.
- [34] T.T.Y. Huang, S. Elekdag-Turk, O. Dalci, et al., The extent of root resorption and tooth movement following the application of ascending and descending magnetic forces: a prospective split mouth, microcomputed-tomography study, *EJO (Eur. J. Orthod.)* 39 (5) (2017) 547–553.
- [35] W.H. Organization, Environmental health criteria 69 magnetic fields, WHO Report (1987) 20–22.
- [36] E.Y. Yiu, D.T. Fang, F.C. Chu, T.W. Chow, Corrosion resistance of iron-platinum magnets, *J. Dent.* 32 (6) (2004) 423–429.